Characterization of the NPOI fringe scanning stroke

Anders M. Jorgensen[a], Dave Mozurkewich[b], James Murphy[c], Marc Sapantaie[c], J. Thomas Armstrong[c], G. Charmaine Gilbreath[c], Robert Hindsley[c], Thomas A. Pauls[c], Henrique Schmitt[c,e], Donald J. Hutter[d]

[a]Los Alamos National Laboratory, Los Alamos, NM, USA
[b]Seabrook Engineering, Seabrook, MD, USA
[c]Naval Research Laboratory, Washington, DC, USA
[d]U.S. Naval Observatory, Flagstaff Station, Flagstaff, AZ, USA
[e]Interferometrics, Inc., Herndon, VA, USA

ABSTRACT

We report on the results of an experiment to characterize the fringe scanning stroke on the Navy Prototype Optical Interferometer (NPOI) Fast Delay Line (FDL) strokes. The measurements were carried out during three days April 11-13, 2005 at the NPOI site near Flagstaff, AZ. The NPOI uses a heterodyne metrology laser system in its operations. It consists of a HeNe laser with a 2 MHz heterodyne component generated by an Acousto-Optic Modulator (AOM). One polarization is used as the 2 MHz clock, and the other is sent through the feed system twice and bounces off the piezo stroke modulators. We sampled both signals at 50 MHz, and obtained stroke and cart combined motion at the frequency of the stroke modulated 2 MHz heterodyne signal. By counting zero-crossings in the reference and feed system signals, a rough position (to a wavelength) can be obtained. This can be further refined to the few-nanometer level by measuring the relative phases of the reference and feed system signals. This results in approximately 4000 positions measurements per 2 ms stroke with a precision of approximately 1 nm. We recorded stroke positions for approximately 500 strokes (1 s), for all but one of the six FDLs, under a variety of conditions: different stroke amplitudes, different cart speeds, and different cart positions in the FDLs. We then analyzed these data from a total of 100 tests to understand the deviation of the actual stroke from the ideal stroke. We found that the mean stroke differs from the ideal stroke, and that consecutive strokes differ from each other. We computed the effect of the non-ideal stroke on the science data. A non-ideal stroke results in leakage of fringe power between fringe frequencies. This leakage is not significant during most normal operations of the NPOI. However, when the squared visibilities of baselines on the same spectrograph differ by large amounts (a factor of 10), care should be taken. Ideally, High- and low-visibility baselines should be placed on different spectrographs.

1. INTRODUCTION

The Navy Prototype Optical Interferometer (NPOI) is located at Lowell Observatory south of Flagstaff, AZ. Its baselines range in length from 2 m to 437 m. 50 cm sidereostats feed 12 cm apertures, and the beam-combining back-end makes measurements in up to 32 wavelength channels between approximately 450 nm and 850 nm. Armstrong (1) has presented a detailed description of the NPOI.

This work concerns the characterization of the linearity and reproducibility of the NPOI fringe scanning stroke which is constructed from stacks of piezo-electric elements. The piezo-electric elements are driven by a high-voltage power supply which nominally produces a triangular waveform with an amplitude of several μm. This scanning shifts the interferometric fringe from the space-domain to the time-domain. Precisely timed data acquisition intervals bin detected photons into one of 64 bins under the assumption of a perfectly triangular fringe-scanning stroke. This paper reports on an experiment conducted to search for and characterize any non-linearities in the fringe-scanning stroke.

This is done by sampling the NPOI 2 MHz heterodyne laser metrology system signals at 50 MHz, and then processing these signals to obtain combined motion of the fringe scanning system and the Fast Delay Line (FDL) carts. The metrology system is a HeNe laser with a heterodyne frequency generated by an Acousto-Optical Modulator. One polarization is used as a timing-signal reference, whereas the other polarization is sent twice through the feed system to bounce off the Piezo-electric elements on the FDL cart. By counting the zero-crossings in the two metrology signals we can get a rough measurement of position to the precision of a wavelength (632.8 nm). By additionally measuring the relative phase of the reference signal and the

[1]Further author information: (Send correspondence to A. M. J.)
A. M. J.: E-mail: andersmjorgensen@yahoo.com, Telephone: 1-505-660-6808

signal that has passed through the feed system, it is possible to achieve nanometer-level precision position measurements. Oversampling the 2 MHz signal significantly allows us to measure the phase difference of the two signals to one part in 600, which corresponds to an approximately 1 nm precision.

2. DATA COLLECTION

We measured the 2 MHz metrology signal for reference and unknown signal separately but synchronized, at a sampling frequency of 50 MHz. The typical measurement length was 1 s, which corresponds to 500 periods of the fringe-scanning stroke. We deemed this sufficient to at least get an initial idea of the state of the stroke. The unknown and reference signal were sampled at 12-bit precision, and those numbers were stored as 2-byte integers in separate files for reference and unknown signal, resulting in approximately 100 MB files for each of the reference and unknown signal, for each test. An example of these signals is plotted in Figure 1. The dotted line represents the reference signal, whereas the solid line represents the unknown signal.

We measured all but one of the FDLs, under different conditions: at different positions in the FDL tanks (front, center, and back), at different cart speeds (0, 1 mm/s, 3 mm/s, and 10 mm/s), and at different stroke amplitudes (-4, -1, 0, 1, 4 μm). We also performed a so-called warm-up test, in which one FDL (FDL #1) was left running stationary for a full day, taking measurements at intervals. The intent of this test was to measure whether the stroke characteristics changed over time. A total of approximately 100 tests were performed.

In this paper we do not reproduce all of the tests, but instead summarize the results. A full report can be obtained from one of the authors (Anders M. Jorgensen, andersmjorgensen@yahoo.com). Table 1 lists just one set of tests, those performed at the front of the FDL tanks, with the carts stationary.

Test name	FDL	stroke (μm)
FDL_2005_04_12_1202	1	0
FDL_2005_04_12_1326	2	0
FDL_2005_04_12_1411	3	0
FDL_2005_04_12_1515	4	0
FDL_2005_04_12_1553	6	0
FDL_2005_04_12_1215	1	1
FDL_2005_04_12_1334	2	1
FDL_2005_04_12_1422	3	1
FDL_2005_04_12_1527	4	1
FDL_2005_04_12_1618	6	1
FDL_2005_04_12_1225	1	4
FDL_2005_04_12_1339	3	4
FDL_2005_04_12_1353	2	4
FDL_2005_04_12_1536	4	4
FDL_2005_04_12_1625	6	4
FDL_2005_04_12_1235	1	-1
FDL_2005_04_12_1403	2	-1
FDL_2005_04_12_1449	3	-1
FDL_2005_04_12_1547	4	-1
FDL_2005_04_12_1627	6	-1
FDL_2005_04_12_1237	1	-4
FDL_2005_04_12_1406	2	-4
FDL_2005_04_12_1451	3	-4
FDL_2005_04_12_1549	4	-4
FDL_2005_04_12_1630	4	-4

Table 1. List of tests performed at front of tank (position 1000 mm) with FDL cart stationary.

3. ANALYSIS

The metrology laser signal can be converted into a position by counting periods of both the reference and the unknown signal. We get one position measurement at each zero-crossing in the unknown signal, which amounts to 2 million position determinations per second, or approximately 4000 per stroke period. The number of position determinations per stroke is only approximate, and positions are irregularly spaced in time, because the time between successive crossings in the unknown signal depends on the speed and direction of motion of the stroke and FDL cart together. In order for this scheme to work reliably, the metrology signals must be stable.

3.1. Stability of the metrology signal.

It is important that the reference signal is stable in order to obtain meaningful stroke position measurements. Figure 2 shows a histogram of the reference time (the time between successive up-crossings) for one file. We have added a Gaussian fit, and the fit is so good that the fitted curve (dashed) almost can not be seen. The dotted curve in Figure 2 is the histogram of time between consecutive up-crossings in the unknown signal. This is for a case in which the cart is moving and the stroke is active, as evidenced by the horizontally displaced double-peaked shape of the histogram. The Gaussian distribution of the reference time suggests that the uncertainty is dominated by discretization of the measurements, as opposed to a non-stable reference signal. Figure 3a plots the average period of the reference signal for all 1-second data sets recorded, as a function of the

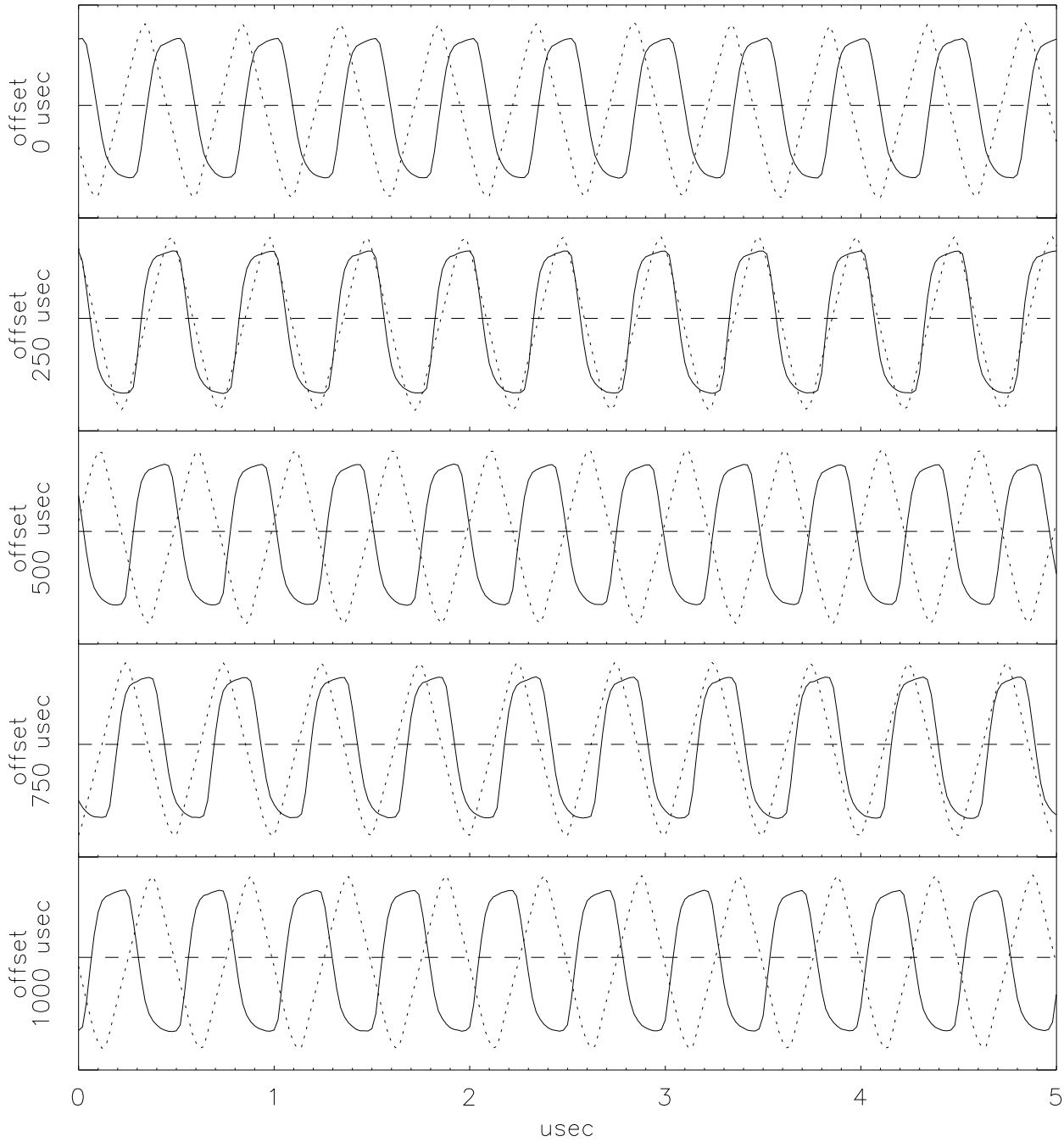

Figure 1. Example of the raw metrology signal. Shown are snapshots of the signals during half of a stroke period. The reference signal (dotted) has constant period and phase, whereas the unknown signal (solid) moves relative to it as the distance to the FDL cart changes.

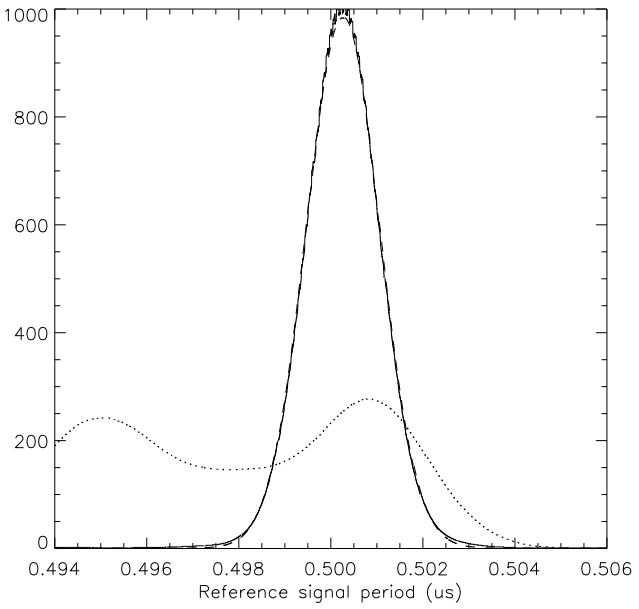

Figure 2. Histogram of the reference time (solid), and of the unknown time (dotted) for test FDL_2005_04_12_1232. A Gaussian fit to the reference time distribution is plotted a dashed curve.

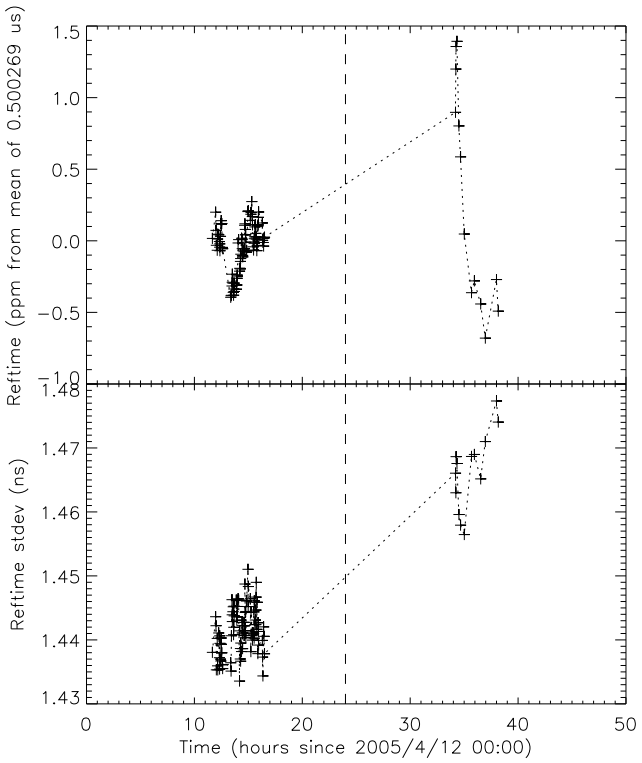

Figure 3. Variation of the average reference time as a function of time the data were recorded.

time that the data were recorded. The variation between individual 1-second experiment is approximately 0.2 parts in 10^6. Figure 3b plots the standard deviation of the reference time for each 1-second experiment. This is the standard deviation of a histogram like the one plotted in Figure 2. In Figure 3 the signals are very stable on the first day of the experiments, while there is some evidence of systematic drift on the second day. However, the drift on the second day is still much smaller than the accuracy which is required for our experiment.

3.2. Computation of metrology position

At each crossing of the unknown signal we can determine the stroke position. From the beginning of the file we maintain a counter, c, which is incremented every time a reference signal crossing is encountered, and decremented every time a unknown signal crossing is encountered. In order to avoid any biases due to the signals not being centered around zero, we count up-going crossings and down-going crossings separately and maintain separate position determinations based on up- and down-going crossings. At each unknown signal crossing we calculate the quantity, d, which is the time since the last reference signal crossing, divided by the time between reference signal crossings. We can then compute the metrology position at each unknown signal crossing via the formula

$$x_m = (c + d)\lambda, \tag{1}$$

where λ is the wavelength of the metrology laser light, 632.8 nm in the case of the NPOI. This gives us approximately 2 million position determinations per second, or approximately 4000 per stroke period.

3.3. Motion subtraction

We subtracted the large-scale motion of the cart through a polynomial fit to the metrology positions as a function of time. It turned out that a linear fit provided the best description of the large-scale motion in all cases. This is reasonable, because the FDL cart speed was programmed to be a constant in all cases. Using a higher-order polynomial for subtracting the cart motion did not work as well.

3.4. Offset subtraction

Subtracting the large-scale motion still leaves a constant offset that must be subtracted. The reason for this is that non-linearities may cause the stroke to not

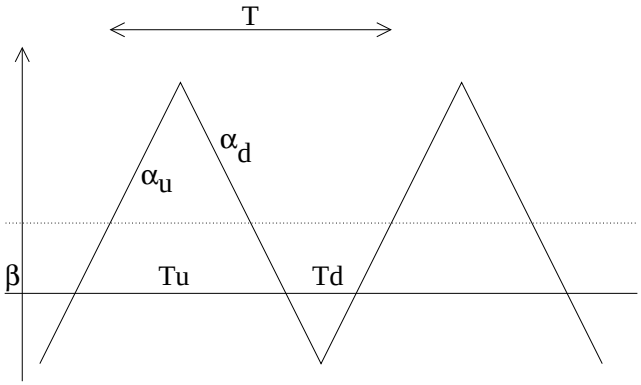

Figure 4. Illustration of the relevant parameters for calculating the offset, β.

be centered around zero even after the large-scale motion has been subtracted. We define the offset to be zero when the average time from up-crossing to down-crossing equals the average time from down-crossing to up-crossing. The calculation of the offset is illustrated in Figure 4. We iterate on this algorithm a few times (up to four), although generally the offset is corrected quite well after just one or two iterations. As can be seen, we need to calculate the time from each up-crossing to the following down-crossing and average those to get T_u. Then we calculate the time from each down-crossing to the following up-crossing, and average those to get T_d. Then at each up-crossing we calculate the slope, and average them to get α_u. The average down-crossing slope is α_d. The offset, β, is then calculated as

$$\beta = \frac{(T_u - T_d)}{2(\alpha_u^{-1} - \alpha_d^{-1})}. \tag{2}$$

The offset subtraction is only accurate to the extent that T_u, T_d, α_u, and α_d are accurately determined. However, the offset-subtraction can be iterated to achieve more accurate offset subtraction. We found that after four iterations the offset subtracted is in the pm range.

3.5. Stroke period and stroke timing

Our data sets did not include measurement of the 500 Hz stroke start pulse. Instead we determine the stroke period and the stroke start time from the data. The stroke period is simply the average of the time between consecutive zero-crossings in the same direction. The stroke start time is a little more complicated. We decide that the stroke start time should be the first up-crossing in the absence of the semi-random noise around the mean stroke. If t_i are the actual stroke crossing times measured in the presence of the noise, then the start of the first stroke, t_0^*, minimizes the sum

$$\sum_i^N |t_0^* + i\delta t - t_i| \tag{3}$$

where there are N crossings, with measured crossing times t_i, and mean stroke time δt. To do this we adjust the first stroke time to be

$$t_0^* = t_0 + \frac{1}{N}\sum_{i=0}^{N-1} t_i - i\delta t + t_0 \tag{4}$$

The stroke start times for all the other strokes are then

$$t_i^* = t_0^* + i\delta t \tag{5}$$

In cases where the stroke is zero, it is not possible to determine any crossings. In that case we just assume a 2 ms stroke.

3.6. Stroke statistics

The last step in the data processing is resampling the strokes on a regular time grid, to calculate average strokes, and RMS variation around the average strokes. The positions must be re-sampled on a regular grid, because we compute the stroke positions only at the times of zero-crossings in the unknown signal. Position information is thus unevenly spaced in time, and we resample it because it simplifies subsequent processing. We resample the approximately 4000 measurements per stroke to 10000 regularly space points per stroke.

In Figures 5 and 6 we show the mean stroke position as well as the variation around the mean stroke position. Based on the number of tests carried out, we could create twenty such plots covering the various measurement conditions, including position of the carts in the FDL tanks as well as speed of travel of the FDL carts. However, we found no evidence that those measurement conditions had any significant effect on the strokes, so that Figures 5 and 6 are representative. Figure 5 shows examples of short strokes (1 μm), and Figure 6 shows examples of long strokes (4 μm). The horizontal dotted lines in the center and bottom panels indicate the number of bins that the variations correspond to, assuming the longest wavelength. The amplitude of the noise in the center panel does not vary much with the amplitude of the stroke, suggesting that it is additive rather than multiplicative. The bottom panel shows a sometimes significant deviation from the ideal stroke. The vertical dashed lines in the bottom panel shows the portion

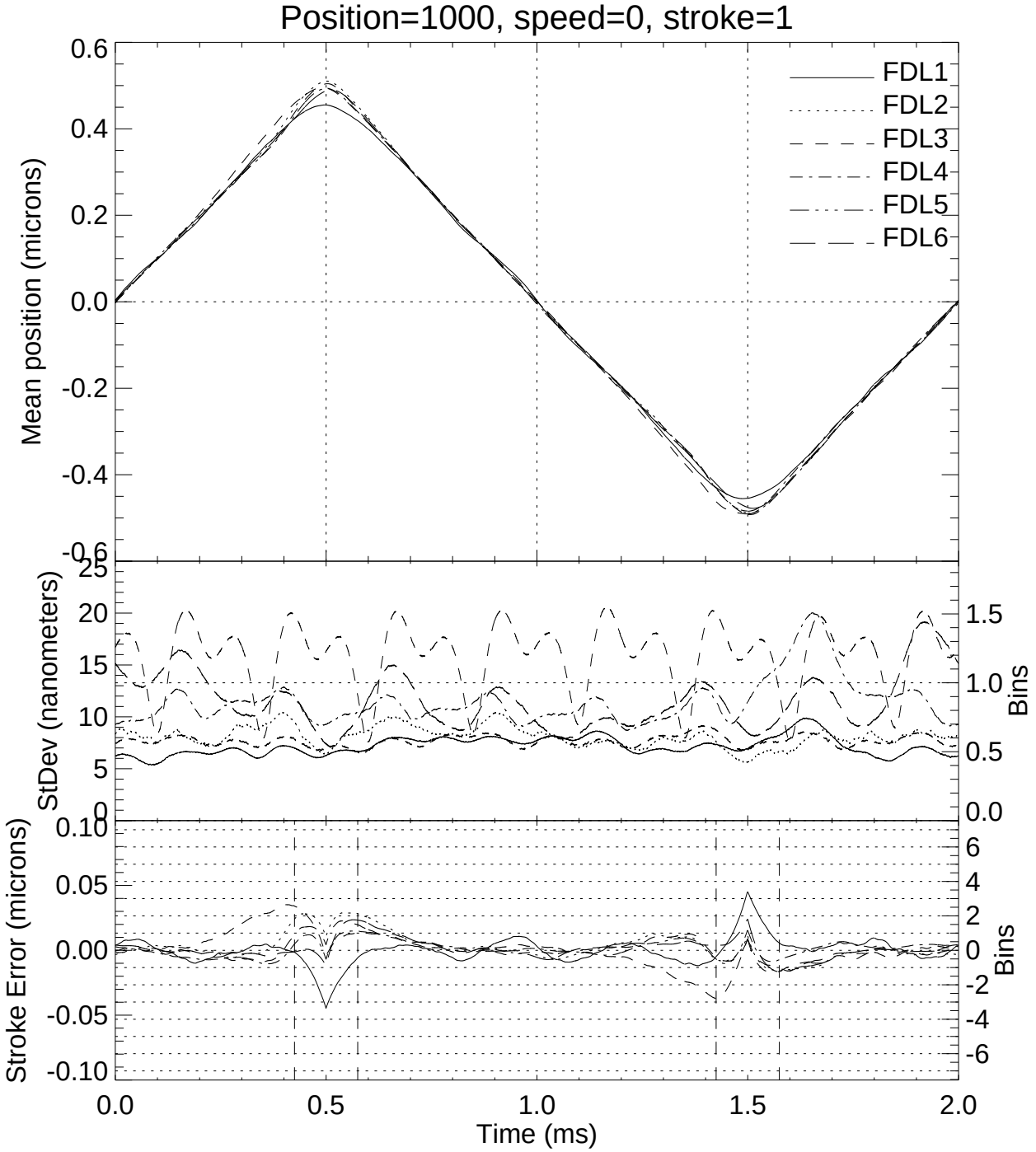

Figure 5. Mean stroke for a 1 μm programmed stroke (top panel), RMS variation around the mean stroke (center panel), and deviation of mean stroke from the ideal stroke (bottom panel) for 5 FDL carts when the cart was stationary at the front of the FDL tanks.

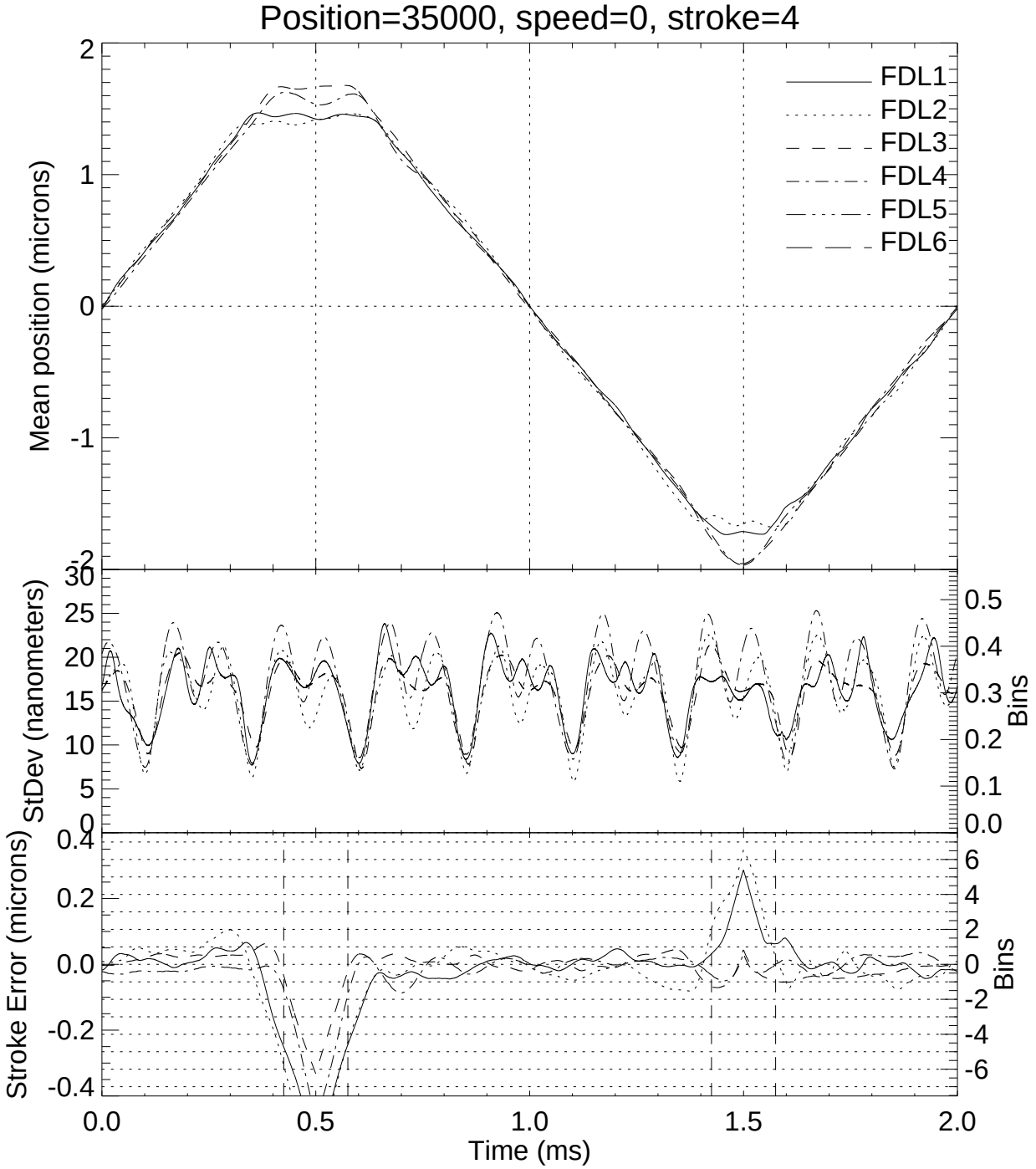

Figure 6. Mean stroke for a 4 μm programmed stroke (top panel), RMS variation around the mean stroke (center panel), and deviation of mean stroke from the ideal stroke (bottom panel) for 5 FDL carts when the cart was stationary at the back of the FDL tanks.

of the stroke which is not used. NPOI data acquisition is timed such that an integer number of wavelengths are sampled. Thus, at the longest wavelength, 0.85 μm, only 85% of the stroke is used, and at the shortest wavelength 0.45 μm, only 45% of the stroke is used. The variation of the stroke from the ideal stroke that occurs between the two sets of dashed lines is therefore not used in data acquisition. Notice also that in Figure 6 the noise around the mean stroke is highly periodic, whereas in Figure 5 we saw less evidence for periodicity. The occurrence of the periodic nature of the noise was not strongly correlated with measurement conditions. However, the fact that it exists suggest that it is in some way tied to the period of the stroke, and that perhaps it is a resonance.

3.7. Stroke power spectra

In order to explore the periodicities and stroke-to-stroke variation we generate the power spectra of the stroke positions. Figures 7 shows the power spectrum of the residual stroke after subtracting the ideal stroke. Each panel shows power spectra for a different position or speed of the FDL cart, and in each panel, there is one curve for each of five stroke amplitudes. The four dotted curves mark the frequencies 500 Hz, 1.7 kHz, 2.3 kHz, and 5.6 kHz. The first is the stroke scanning frequency, and the other three are noise resonances. These three peaks appear to always be present, in all FDLs, and for all conditions, and at the same frequency. The flattening of the spectrum above several kHz represents the digitization noise in the measurement.

3.8. Warm-up

The warm-up test was conducted in order to understand whether the piezos would settle into a mode of lower stroke-to-stroke variation after operating at a constant stroke for some period of time. Figure 8 shows the change in the mean stroke between consecutive measurements of the stroke, as a function of time since the stroke was first set. Clearly, the change in the mean stroke with time decreases the longer the stroke is left. We attribute this to the piezos warming up and settling into a mode of consistent repeatable operation, as average over 1 second. Figure 9 shows the RMS of the rate of change of the mean stroke as a function of time. After less than 10 minutes, the rate of change in the mean stroke is less than the RMS noise variation around the mean stroke in our typical measurements. After one hour it has decreased to about 2 nm/hour. Figure 10 shows the average up- and down-slopes of the stroke as a function of time. In the first few minutes, there is some variation of the slope relative to the ideal value of

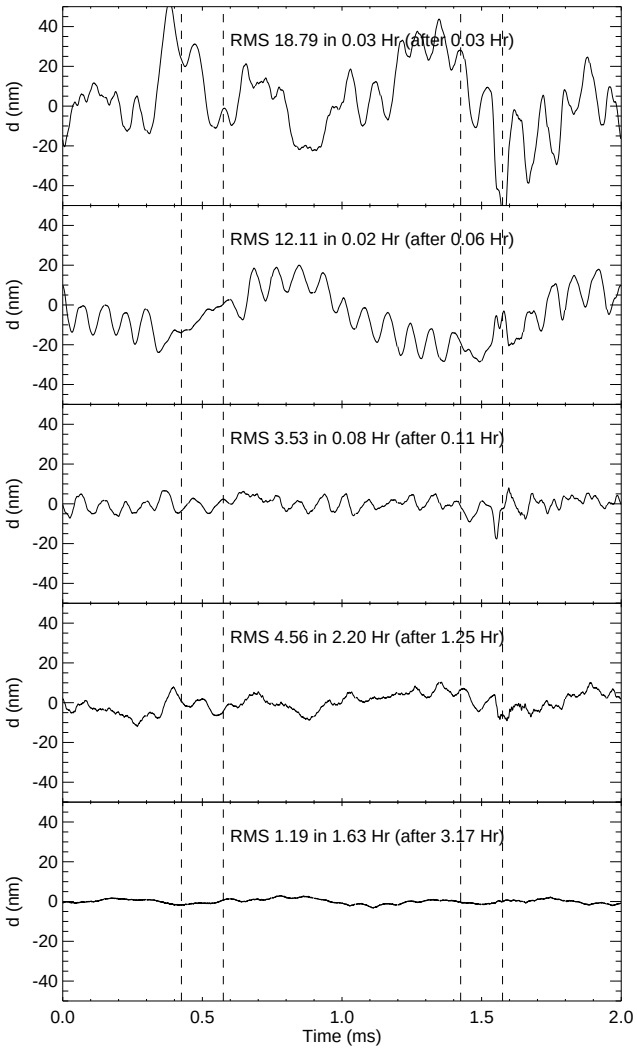

Figure 8. Change in mean stroke between consecutive measurement of the stroke. In each panel is also listed the RMS of this variation over the used range of the stroke.

4 μm, but the slopes appear to settle to values slightly less than 4 μm after the first 10 minutes. The current operating procedure at NPOI is to set the strokes an hour before observing begins to allow them to warm up and settle. According to these measurements, that procedure appears to work well in eliminating most of the short-term variation in the stroke during measurements. This also suggests that non-linearities in the mean stroke are due to non-linearities in the response of the piezos to applied voltage, and thus can be corrected for by modifying the applied voltage across the piezos. Such corrections have in fact been applied to the NPOI piezos, but as piezos age, their response may change, necessitating that regular recalibrations of the strokes

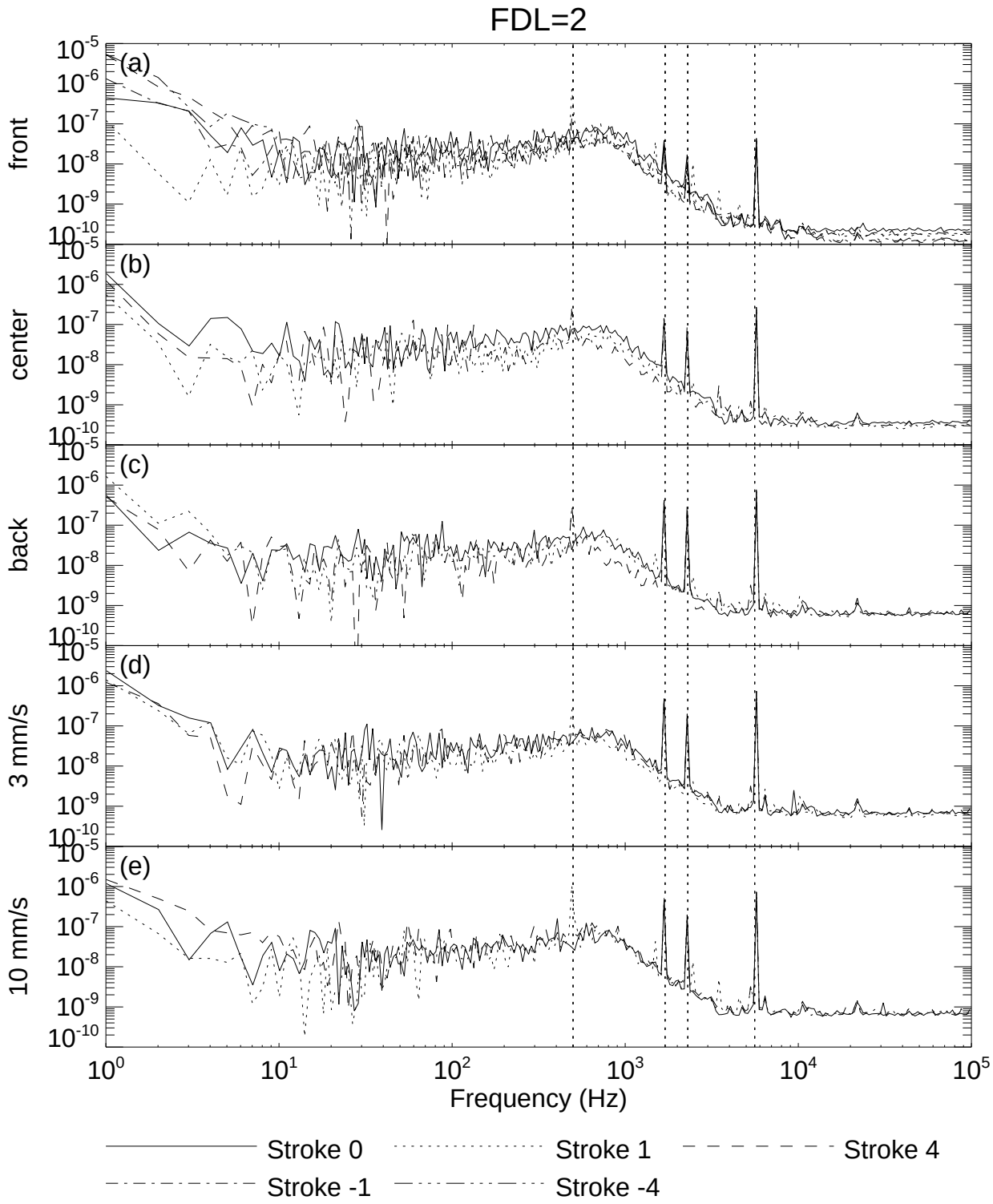

Figure 7. Power spectra of all position measurements for FDL 2, sorted by measurement condition. From top to bottom, the panels show power spectra for the three stationary positions of the FDL cart, and then for the two speeds of the cart. In each panel, there is one curve for each of five stroke amplitudes, 0, 1, 4, -1, and -4 μm. The vertical dotted lines mark 500 Hz (the stroke frequency), 1.7 kHz, 2.3 kHz, and 5.6 kHz.

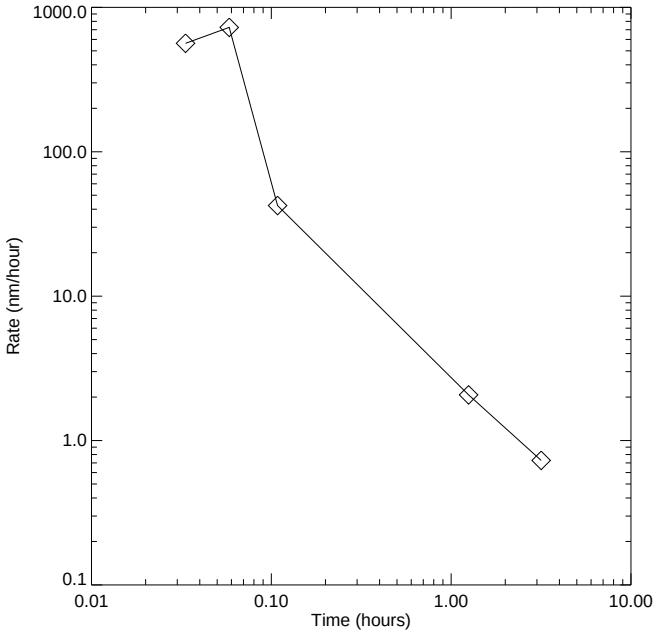

Figure 9. RMS of the rate of change of the mean stroke, as a function of time.

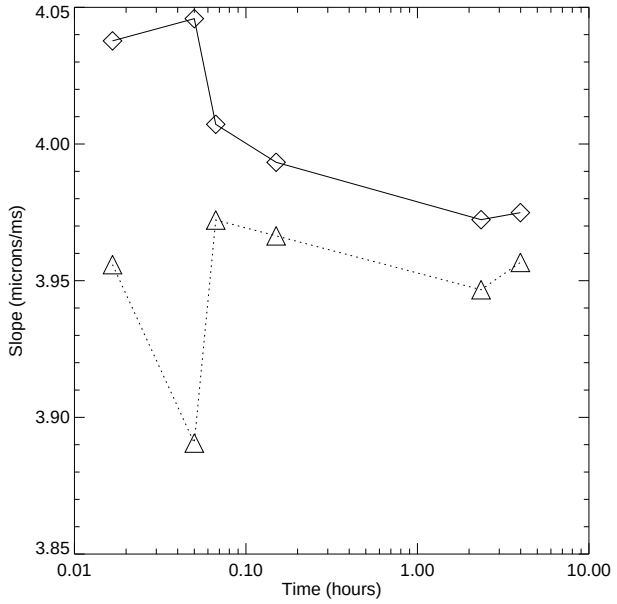

Figure 10. Mean stroke slopes as a function of time. The solid curve is the slope of the up-stroke, and the dotted curve is the negative of the slope of the down-stroke.

may be necessary.

4. EFFECT ON SCIENCE DATA

In order to determine the effects of the stroke errors on the science data, we simulated data sets using the measured strokes, at a variety of frequencies, using appropriate combinations of measured strokes. For example to produce a data set with fringe frequency two, we can combine two amplitude 1 strokes, or two amplitude -1 strokes. To produce a data set with fringe frequency 3 we can combine an amplitude 1 stroke with an amplitude -4 stroke, or an amplitude -1 stroke with an amplitude 4 stroke. Once we have created the data set we compute the power spectrum for all fringe frequencies. In the case of an ideal stroke we should see power only at the original input frequency. In the case of a non-ideal stroke, we should also expect to see power at other fringe frequencies. Figures 11 and 12 show the power spectrum for fringe frequencies 3 and 8 respectively. Recall that there are two ways in which we can produce a given fringe frequency, creating both a positive and a negative stroke. In reality there are many more ways to do it because we can pick any pair of stroke amplitudes for any measurement conditions for any set of two FDLs. The contents of these two plots are just examples of the types of power spectra that we can see. The solid curves show the power spectrum produced by using the actual measured stroke for 1 second of data, which is 500 stroke periods. There are two solid curves, because we picked two combinations, one with a positive combined stroke, and one with a negative combined stroke. To be fully representative, we should perform this computation for all possible combinations of FDLs and measurements conditions which produce the correct combined stroke. In the case of fringe frequency 3, Figure 11, we see that there is leakage into adjacent fringe frequencies (2 and 4) at the level of a few percent, and that leaked power drops further as we go to higher fringe frequencies. In the case of fringe Frequency 8, Figure 12, the power leakage into fringe frequency 9 is a little larger, perhaps as large as 7 or 8%. There is also leakage into lower frequencies at the level of 5-6%.

We also looked at the effects of the average nonlinearity and the noise separately as a sources of power leakage. The dotted curves show the effects of the average stroke only. We generated this by repeating the simulation setting all strokes equal to the average stroke. The dashed curve shows the effects of the noise only on the power leakage. The noise is the RMS variation from stroke to stroke. To generate this we added the

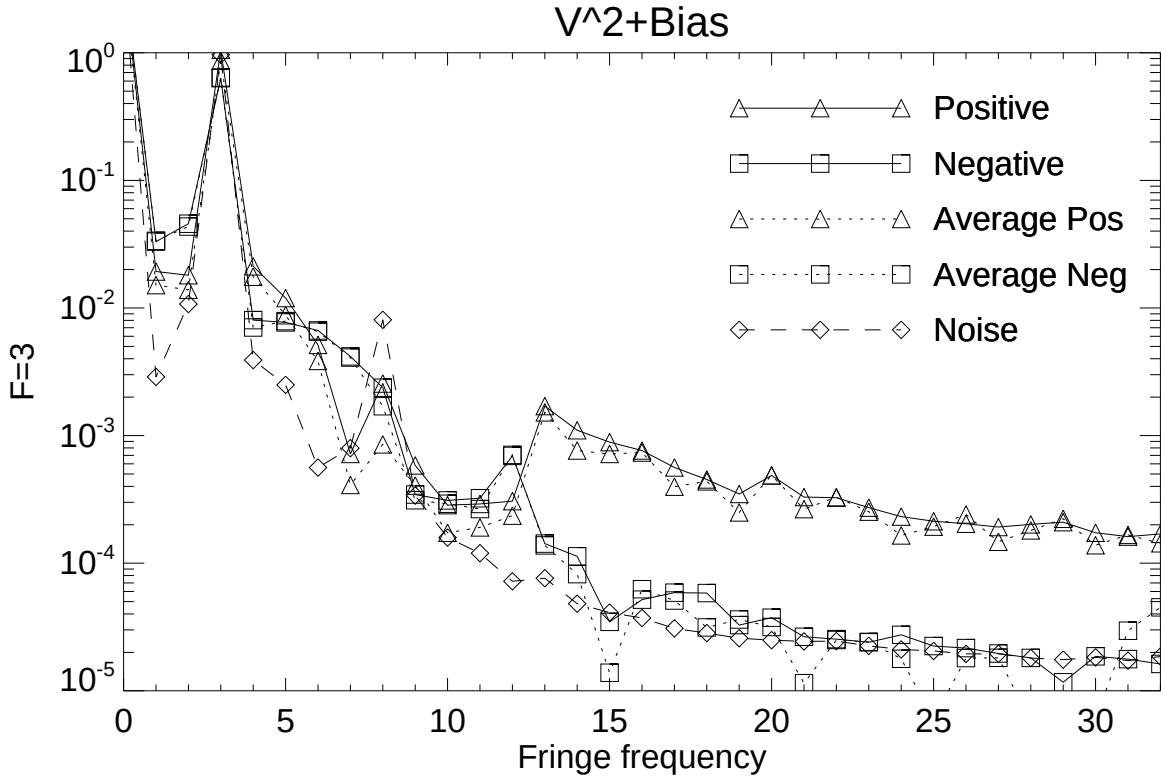

Figure 11. Fringe power spectrum for an input fringe frequency of 3.

noise of a nominally zero-stroke data set to a synthetic ideal stroke. What we notice from these two simulations is that non-linearities in the mean stroke are far more important in generating power leakage than the noise. This is good news, because it is probably much easier to correct the mean stroke than it is to eliminate the noise.

We find that cross-talk at adjacent frequencies is usually not a big problem when all baselines have similar visibility amplitudes, but that it can be a problem when one baseline has significantly smaller visibility amplitude than other baselines. The amount of cross-talk power from a baseline A to a baseline B is directly proportional to the power on baseline A. Thus if baseline A has large power, and baseline B has small power, the cross-talk from baseline A will be a relatively large fraction of the true signal on baseline B.

5. DISCUSSION

We have characterized the NPOI strokes, their time-variation, and the effects of non-linearities of the stroke on science data, and cross-talk, or leakage between fringe frequencies on the same detector. For most high-visibility operations, the leakage of fringe power between fringe frequencies is probably not a major concern because this power leakage will appear primarily as a relatively small bias. When observing low visibility fringes, for example through bootstrapping, it is necessary to consider the effects of leakage between fringe frequencies. For a typical small visibility of 0.1 or less, the leakage from an adjacent fringe frequency can be comparable to the signal. The effects of leakage can be minimized, and perhaps almost eliminated by placing baselines with very different amplitudes on different spectrographs, or at least by separating them widely in fringe frequencies. It appears that the leakage from a fringe frequency is minimized at significantly higher frequency. In the case of NPOI it would therefore be ideal to place the highest visibility baselines, which are often used for tracking in a bootstrapping scenario, at the lowest frequencies, and placing the bootstrapped low visibility baseline at a much higher fringe frequency. When calibrating visibilities the leakage pattern may be different, because the distribution of visibility amplitudes changes. The fact that non-linearities of the strokes dominate over noise by an order of magnitude

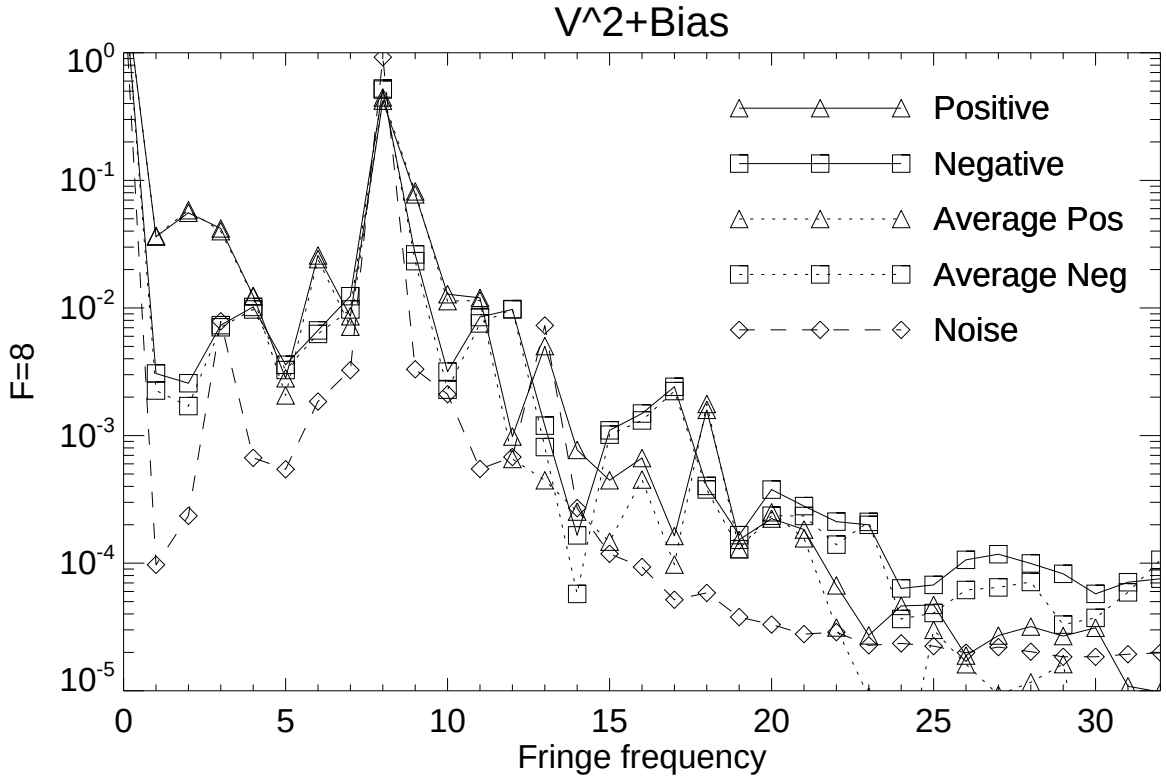

Figure 12. Fringe power spectrum for an input fringe frequency of 8.

means that the majority of the leakage can be eliminated by carefully measuring the stroke and compensating for the non-linearities in the the controlling voltage. Once set and warmed, the stroke appears long-term stable, suggesting that infrequent stroke measurements and corrections can significantly reduce the leakage.

6. CONCLUSION

Interferometers such as NPOI are coming online with the ability to bootstrap baselines, and thus indirectly track fringes on baselines with very small visibilities. Piezo strokes should be monitored and taken into account during data acquisition or during analysis, or steps should be taken to minimize the effects of the cross-talk. The effect of cross-talk can be minimized either by placing different baselines on different detectors, at least placing the low-visibility science baselines on a separate detector from the high-visibility tracking baselines, or by encoding different baselines at fringe frequencies spaced far apart.

It would be prudent for future interferometers to implement a mechanism for frequently monitoring and correcting the fringe scanning stroke.

ACKNOWLEDGMENTS

The NPOI is funded by the Office of Naval Research and the Oceanographer of the Navy. This work was also supported by the U.S. Department of Energy and the University of California. The authors would like to thank Brit O'Neill and Jim Benson for their assistance in carrying out the experiments.

REFERENCES

1. J. T. Armstrong, D. Mozurkewich, L. J. Rickard, D. J. Hutter, J. A. Benson, P. F. Bowers, N. M. Elias II, C. A. Hummel, K. J. Johnston, D. F. Buscher, J. H. Clark III, L. Ha, L.-C. Ling, N. M. White, and R. S. Simon, "The Navy Prototype Optical Interferometer," Astrophys. J. **496**, pp. 550–571, 1998.